



Evidence of NAO control on subsurface ice accumulation in a 1200 yr old cave-ice sequence, St. Livres ice cave, Switzerland

Markus Stoffel^{a,b,c,*}, Marc Luetscher^{d,e}, Michelle Bollschweiler^{b,c}, Frédéric Schlatter^c

^a Climatic Change and Climate Impacts Group (C3i), Institute for Environmental Sciences, University of Geneva, Site de Batelle, chemin de Drize 7, CH-1227 Carouge-Geneva, Switzerland

^b Laboratory of Dendrogeomorphology (Dendrolab.ch), Institute of Geological Sciences, University of Berne, Baltzerstrasse 1 +3, CH-3012 Berne, Switzerland

^c Department of Geosciences, Geography, University of Fribourg, chemin du Musée 4, CH-1700 Fribourg, Switzerland

^d Geology and Paleontology, University of Innsbruck, Innrain 52, A-6020 Innsbruck, Austria

^e Swiss Institute for Speleology and Karst Studies (SISKA), P.O. Box 818, CH-2301 La Chaux-de-Fonds, Switzerland

ARTICLE INFO

Article history:

Received 15 September 2008

Available online 16 April 2009

Keywords:

Cave ice

Sporadic permafrost

Dendrochronology

Radiocarbon dating

North Atlantic Oscillation (NAO)

Picea abies (L.) Karst.

ABSTRACT

Mid-latitude ice caves are assumed to be highly sensitive to climatic changes and thus represent a potentially interesting environmental archive. Establishing a precise chronology is, however, a prerequisite for the understanding of processes driving the cave-ice mass balance and thus allows a paleoenvironmental interpretation. At St. Livres ice cave (Jura Mountains, Switzerland), subfossil trees and organic material are abundant in the cave-ice deposit, therefore allowing the dating of individual ice layers. The dendrochronological analysis of 45 subfossil samples of Norway spruce (*Picea abies* (L.) Karst.) from the overhanging front of the ice outcrop as well as the dating of seven wood samples with ¹⁴C dating allowed for a reconstruction of the St. Livres cave-ice sequence and for the determination of periods of ice accumulation and ablation. Results suggest a maximal age of 1200 ± 50 ¹⁴C yr BP for the observed ice sequence and indicate the presence of four major deposition gaps dated to the 14th, 15th, mid-19th and late 19th century, which can be related with periods of positive North Atlantic Oscillation anomalies (NAO+) over the winter half-year and/or anthropogenic cave-ice abstraction. Similarly, there is evidence that periods of cave-ice accumulation as observed between AD 1877–1900 and AD 1393–1415 would correspond with phases of negative NAO indices. Cave ice represents therefore an original climate archive for the winter half-year and is complementary to other continental proxies recording preferentially summer conditions (e.g., tree rings, varves).

© 2009 University of Washington. Published by Elsevier Inc. All rights reserved.

Introduction

Mid-latitude ice accumulations raise increasing interest for paleoenvironmental research as they are often located close to highly populated and industrialized areas (e.g., Cecil et al., 2004). High-altitude Alpine glaciers have proved to be suitable archives for the study of recent changes in the composition of atmospheric gases (e.g., Schwikowski et al., 2004). Miniature ice caps on mountain crests frozen to the bedrock or perennial ice patches frozen to the permafrost represent another type of cold alpine bodies expected to contain well preserved, old ice (Haeberli et al., 2004). Finally, mid-latitude/low-altitude cave-ice deposits are supposed to represent an original archive for the winter half-year and thus to be complementary to other paleoenvironmental proxies (Luetscher et al., 2005). Sometimes located at altitudes well below the 0°C-isotherm, these ice caves could provide valuable paleoclimatic data in regions where proxies or instrumental records are often missing.

Although the potential of ice caves for paleoclimate studies has been underlined by several authors in the past (e.g., Yonge and MacDonald, 1999; Holmlund et al., 2005), there is only very little information available on the time window accessible in cave-ice outcrops. Most authors agree that low-altitude cave ice in temperate regions results from current accumulation processes, but mass turnover rates can vary significantly from one cave to the other. For instance, recent studies carried out in Monlési ice cave (Jura Mountains, Switzerland) highlight an enhanced mass turnover rate with the oldest ice layers being only 120 yr old (Luetscher et al., 2007). In contrast, investigations completed in Central Europe (e.g. Scarioara ice cave; Holmlund et al., 2005) or North America (e.g., Nahanni ice cave; Schroeder, 1977) yielded radiocarbon evidence for the presence of significantly older cave-ice deposits.

Although radiocarbon ages from organic material trapped in cave-ice outcrops were reported from various study sites, results are often based on unique samples and only a limited number of detailed cave-ice chronostratigraphies has been published so far (e.g. Holmlund et al., 2005, Clausen et al., 2007, Kern et al., 2007, Luetscher et al., 2007). Yet, paleoenvironmental interpretations can be achieved only when based on a reliable age model, indispensable to assess the continuity of the record. Through the dendrochronological dating of one of the

* Corresponding author. Climatic Change and Climate Impacts Group (C3i), Institute for Environmental Sciences, University of Geneva, Site de Batelle, chemin de Drize 7, CH-1227 Carouge-Geneva, Switzerland.

E-mail address: markus.stoffel@unifr.ch (M. Stoffel).

largest ice deposits known in the Jura Mountains, this study illustrates the formation of cave ice over the last 1200 yr and indicates the presence of major hiatuses in the accumulation sequence. Besides contributing to the understanding of the local depositional context, results may also help the identification of extreme events, which could be cross-validated with climate proxies on e.g., North Atlantic Oscillation (NAO) indices (Cook et al., 2002) or temperature and precipitation data (Pfister, 1999).

Study site

The Jura Mountains form an approximately 400 km wide arc between the Savoie region (France) in the southwest and the Black Forest (Germany) in the northeast. Largely consisting of carbonate rocks, most of the Jura Arc is affected by intense karstification processes (e.g., Aubert, 1969). The inner part of this NW arcuate range, mostly located in Switzerland, is characterized by a succession of crests and valleys ranging between 1000 and 1500 m above sea level (m a.s.l.), with the highest peaks reaching about 1700 m a.s.l. Mean annual air temperatures measured at these altitudes vary between 6.5 and 3.5°C. Maximum annual temperature amplitudes reach up to 50°C, while a difference of 17°C between the warmest and the coldest months is common (MeteoSwiss, 2008). The temperate climate of the Jura Mountains is strongly influenced by oceanic meteorological conditions. As a first obstacle from the Atlantic Ocean, the Jura Mountains benefit from abundant precipitation, usually between 1200 and 1600 mm yr⁻¹, which can reach more than 2000 mm yr⁻¹ on certain crests (MeteoSwiss, 2008). Snow precipitation occurs about 50 days yr⁻¹ on the higher summits and represents half of the total yearly precipitation observed. The accumulation of snow can locally reach more than 2 m and snow remains from November to May in

certain “combes” (= small valleys) of the high range. The regional vegetation is largely dominated by Norway spruce (*Picea abies* (L.) Karst.), but Silver fir (*Abies alba* Mill.), Common beech (*Fagus sylvatica* L.), Great maple (*Acer pseudoplatanus* L.) and Mountain ash (*Sorbus aucuparia* L.) are observed as well (Buttler et al., 2001).

Although the Jura Mountains do not belong to the commonly recognized permafrost occurrences of Switzerland (Keller et al., 1998), 25 perennial cave-ice fillings were identified in the area (Luetscher et al., 2005). The St. Livres ice cave has been selected for detailed investigations because of the large amounts of massive ice, visible and accessible ice stratification, the presence of considerable amounts of woody debris and its good speleological documentation (Audéat et al., 2002). The cave is located at 1359 m a.s.l. in the western part of the inner Jura range (Bière, Vaud, 6°17'50"/46°33'47") and opens within a grove on the south-facing slope of a closed depression. A large collapsed doline (diameter = ~20 m) forms the unique entrance of this cave and leads to the deepest part of the cavity at -45 m (Fig. 1). This downsloping conduit acts as a thermal trap where convective air circulation is restricted to the winter season. When the external temperature falls below the cave air temperature, a strong bidirectional density driven air flow cools the system allowing the formation and preservation of cave ice. In contrast, the summer season is characterized by the absence of any significant subsurface air circulation and direct solar radiation barely reaches the cave interior. The higher density of the cold cave air therefore induces a thermal stratification resulting in a negative annual temperature anomaly as compared to the external atmosphere.

A volume of ice, estimated at about 1200 m³, occupies the base of the entrance shaft. It results essentially from the diagenesis of snow (i.e. firn) accumulated during winter, but local refreezing processes of infiltration water also contribute to the actual ice mass. The cave-ice

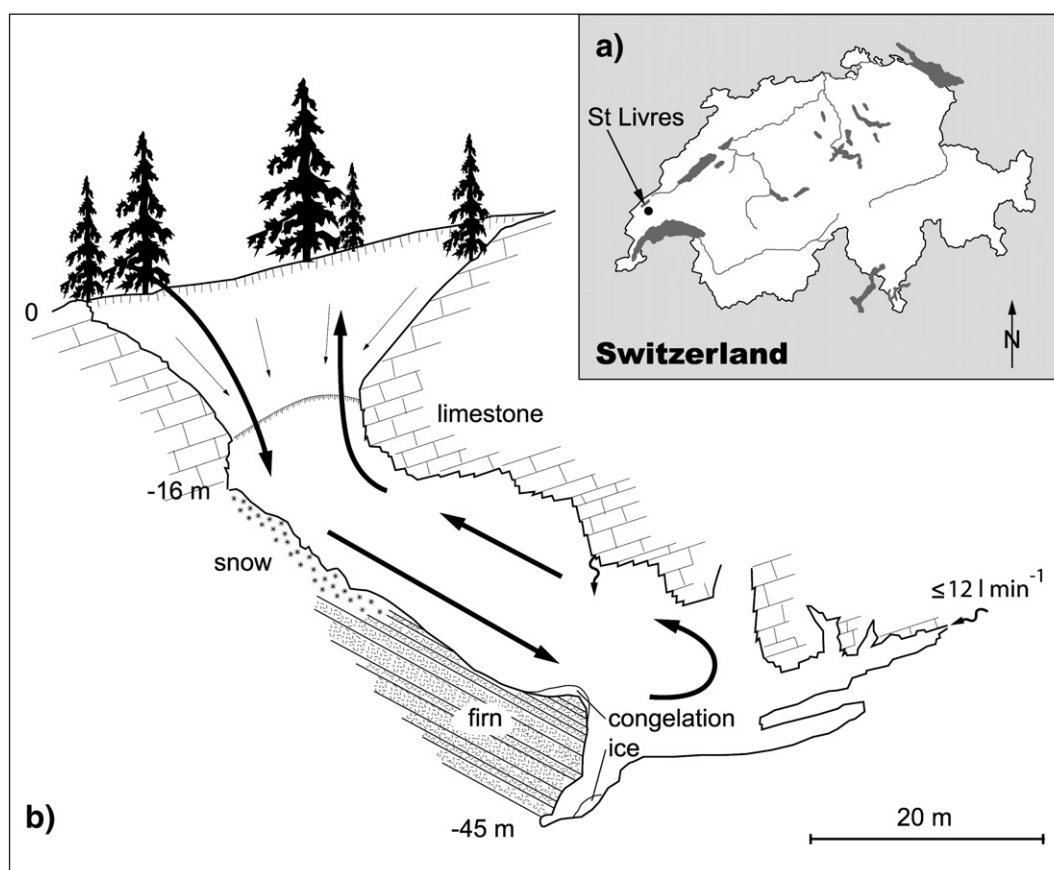


Figure 1. (a) Location and (b) vertical cross-section of St. Livres ice cave. Air circulation during the winter season is shown by bold arrows. The 1200 m³ ice volume is preserved in this cave despite a mean annual air temperature of 4.5°C. The subfossil wood samples selected at St. Livres originate from the ice front at the bottom of the cave.

volume reaches its annual maximum during spring, from which point heat exchanges with the surrounding environment induce a net ablation. The resulting balance determines the thickness of annual ice strata deposited in the cave. For the last few years however, a strong negative mass balance has been observed, which is attributed both to a decrease in winter snow precipitation and warmer temperatures (Luetscher et al., 2005).

While heat exchanges with the external atmosphere control the cave-ice mass balance at the base of the entrance shaft, the development of the subsurface ice volume is mainly controlled by a temporary water inlet (up to 12 l min^{-1}) located at the extremity of the cave. The enhanced ablation front associated with this water inlet induces a gravitational ice flow from the accumulation zone at the base of the entrance shaft to the lower part of the cave. This flow transports detrital material comprising organic deposits (leaves, twigs, branches and trunks) accumulated during storm events in the summer/autumn season and cryoclastic rock fragments leading to the formation of small-scale moraines. This detrital material also delineates the ice stratification observed at the ice front, and thus represents an interesting proxy for the identification and dating of past phases of cave-ice accumulation/ablation.

Materials and methods

Cave-ice lithostratigraphy

Cave-ice lithologies were distinguished according to their macroscopic structure and singular layers were identified based on their content in organic material. The two-dimensional stratigraphic mapping of the ice front was achieved in the field with the benefit of a photomontage involving 13 individual pictures. Subfossil wood samples were located in or on the ice layers using a Leica theodolite equipped with a laser distance meter. Final accuracy of positioning was assessed at $\pm 5 \text{ cm}$. Stratigraphic dipping was measured using a Suunto sighting clinometer with an accuracy of $\pm 1 \text{ gon}$ (i.e. $1 \text{ gon} = \pi/200$).

Dendrochronological dating of subfossil trees

Cross-sections were sawn from *P. abies* trunks or branches identified in or on the ice layers. In the laboratory, samples were dried before processing according to standard dendrochronological procedures (Stokes and Smiley, 1968; Bräker, 2002). Individual working steps included (i) sanding of cross-section surfaces so as to enhance visibility of the cellular structure of the wood; (ii) counting of increment rings; (iii) realizing skeleton plots; (iv) measuring ring widths to the nearest 0.01 mm with a sliding table and a Leica stereo microscope connected to a computer; before (v) building mean growth curves from the two radii measured per individual cross-section. In total, 45 cross-sections were prepared from *P. abies* trunks and large branches present in the frontal area of the ice body or at its surface.

Results were compared with a reference chronology built from trees growing outside the ice cave to cross-date the subfossil trees in the cave with living specimens. We therefore sampled 52 increment cores of 26 *P. abies* trees growing in the loose forest stand neighboring the ice cave (sampling height $\approx 130 \text{ cm}$). Selection of trees for the reference chronology was based on two criteria: (i) absence of obvious signs of injuries or disease so as to minimize non-climatic influences on ring growth; and (ii) tallest and largest diameter in order to maximize the ages of sampled trees and the length of the tree-ring chronology. Each ring-width measurement series was indexed and standardized (i.e. generation of growth indices through the fitting of curves to growth series) in order to remove age trends or effects of stand dynamics (Cook and Kairiukstis, 1990; Vaganov et al., 2006). Mean growth curves were built per tree and all mean curves were summarized to one reference chronology.

The length of the local chronology was limited to the time period with a sample size of at least five trees to guarantee adequacy of sample replication in the early years of the chronology where the number of the samples is usually smaller than in the more recent period (see Wigley et al., 1984). Consequently, the total length of the local chronology was limited to the period AD 1789–2003. As radiocarbon data indicated high ice-layer ages, we complemented our chronology and extended it back to AD 1200 by using a regional reference curve compiled by the Neuchâtel Archaeology Service (Egger et al., 1985; Gassmann, 2007). The latter is built from living trees and fossil wood originating from the larger study site region.

Mean ring-width series of the ice-cave samples were graphically and statistically compared with the local and regional reference chronologies. Graphical comparison included overlay plotting of mean growth curves derived from the subfossil samples with the reference chronologies. Statistical procedures included a cross-date index (CDI; Rinn, 1989) and the analysis of so-called parallelisms ('Gleichläufigkeit' or *W* statistics, *Glk*; see Eckstein and Bauch, 1969; Schweingruber, 1983) between any subfossil series and the reference chronologies as suggested by the Time Series Analysis and Presentation software (TSAP; Rinntech, 2008). Thereafter, the cross-dating accuracy between ring-width series of individual subfossil trees and reference chronologies was evaluated with the Cofecha software (see Holmes, 1983, Grissino-Mayer, 2001).

In order to minimize inaccurate dating of subfossil trees, reconstructed outer-ring ages were only accepted if the dating was based on at least four of the six criteria listed hereafter: (i) length of the tree-ring series $\geq 40 \text{ yr}$; (ii) maximum overlap between the series of the subfossil sample and the chronologies; (iii) parallelism (*Glk*) $\geq 65\%$ between the subfossil sample series and the reference chronologies; (iv) cross-date index (CDI) ≥ 100 ; (v) Cofecha correlation value $p \geq 0.4$; (vi) results confirmed by both chronologies for samples with an inner-ring age younger than AD 1789 (i.e. period covered by both chronologies). Differences in the quality of precisely dated outer-ring ages are presented with a confidence level where three stars (***) indicate the dated samples fulfilling all criteria, whereas two stars (**) and one star (*) stand for those subfossil trees responding to five and four of the criteria, respectively. Those samples failing to fulfill at least four of the criteria were not considered for further analysis.

Radiocarbon dating of subfossil trees and organic litter

To validate and extend the chronostratigraphy of the St. Livres ice cave, seven additional ^{14}C analyses were performed at the accelerator mass spectrometry (AMS) laboratory of the Swiss Federal Institute of Technology Zurich (ETHZ) by measuring the $^{14}\text{C}/^{12}\text{C}$ ratio. Wood samples were pre-treated in a Soxhlet apparatus, using hexane, acetone and ethanol, followed by the standard acid-alkali-acid treatment. The procedure described by Vogel et al. (1984) was used for graphitization. Calibration of the ^{14}C ages was performed using the CalibETH program (Niklaus et al., 1992) and ages are given with a 2σ confidence interval.

Results

Cave-ice lithostratigraphy

The cave-ice outcrop under investigation consists of a slightly overhanging ice front of about $15 \times 8 \text{ m}$, more or less oriented north-south (Fig. 2). A complex sedimentary profile is observed at this ice front showing an interstratification between two main lithologies. The first, described hereafter as "congelation ice," consists of thin-layered orientated centimeter-size ice crystals attributed to individual freezing events associated with specific recharge events (snowmelt and rainfall). These congelation ice layers are between 0.5 and 2 cm thick

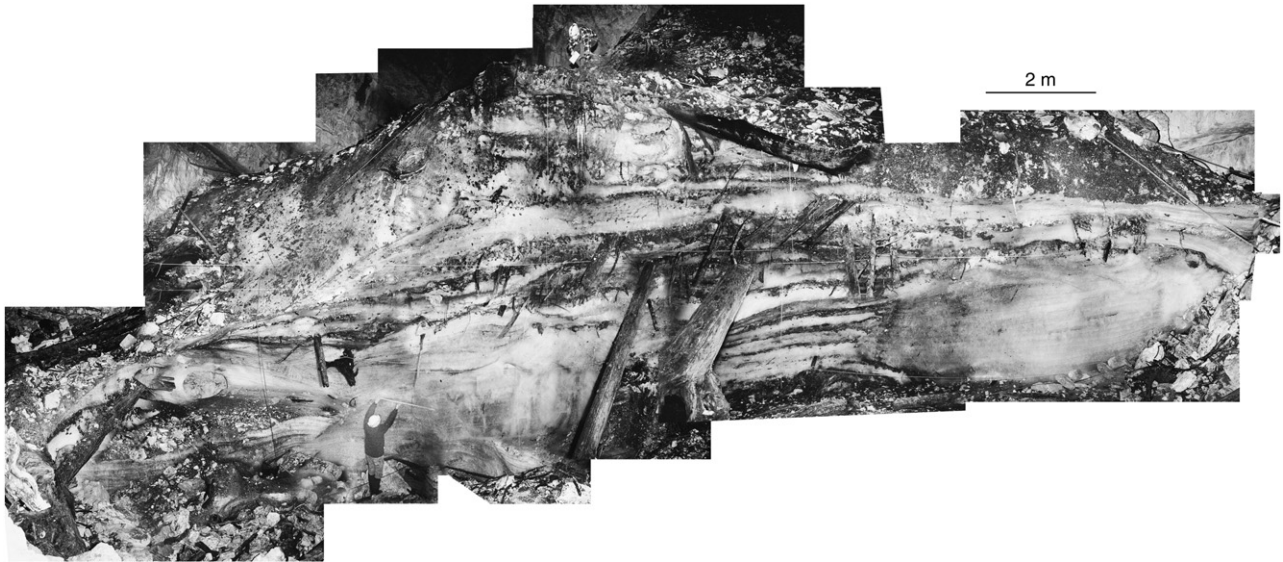


Figure 2. Photomontage of the present-day ice front with the characteristic organic deposits (with trunks, branches, cones and litter) between individual firn ice accumulations and the thin-layered, almost organic-free congelation ice formations (© R. Wenger, SISKKA, used with permission).

and well distinguishable *in situ*, because of their transparency and strong absorption of light. They are sometimes associated with a thin deposit of cryogenic cave calcite formed by the segregation of solutes during freezing. In contrast, “firn ice” has an isotropic structure comprising of coarse equidimensional grains, and thus tends to be opaque and reflective. Strong recrystallization due to repeated melting and freezing implies a high density of firn ice which lies within the uncertainty range of congelation ice fabrics. Firn layers (2–50 cm in thickness) are mostly parallel to the substratum and contain frequent organic clasts in their upper section. They are sometimes associated with decimeter-sized angular rock fragments issued from frost shattering of the cave walls. This detrital material may be sufficient to form singular layers which are often related to a negative cave-ice mass balance over a period of several years. Therefore, detrital layers represent a useful marker to underline distinct phases of cave-ice accumulation. A total of six individual stratigraphic units separated from each other either by erosive, intrusive or sedimentary contacts is observed at the front of the St. Livres ice cave (Fig. 3):

The 260 cm thick *Unit 1* is positioned at the base of the cave-ice sequence. It consists of congelation ice and a minimum of 65 laminations which thicknesses range from 1–5 cm. The ice layers

are deposited parallel to the substratum and contain only very little organo-clastic material. *Unit 1* is delimited from adjacent units by an erosive contact. While the lower part is prograding onto *Unit 2*, the upper part is truncated by a decimetric layer (*S14*) rich in organic material being in stratigraphic discordance.

Unit 2 comprises a 220 cm thick firn deposit characterized by 13 individual layers (4–35 cm in thickness, labeled *S1* to *S13* in Fig. 4), separated from each other by organic material. Organic deposits consist mainly of twigs and small branches of *P. abies* and *F. sylvatica*. The ice layers appear to be in sedimentary concordance and some cross-stratifications are observed as well. *Unit 2* overlies some remobilized material such as stems and planks which are not in stratigraphic concordance. At both ends, it has an erosive contact with the adjacent *Units 1* and 3, but is in sedimentary concordance with the truncating layer *S14*.

Unit 3 consists of translucent congelation ice deposited in centimetric laminae and contains at least 70 strata in the upper half of the outcrop. The presence of organic material is limited to a few twigs. It is delimited from adjacent units by an erosive contact and the upper surface is characterized by a thin muddy deposit which is in stratigraphic discordance with the truncating layer *S18*.

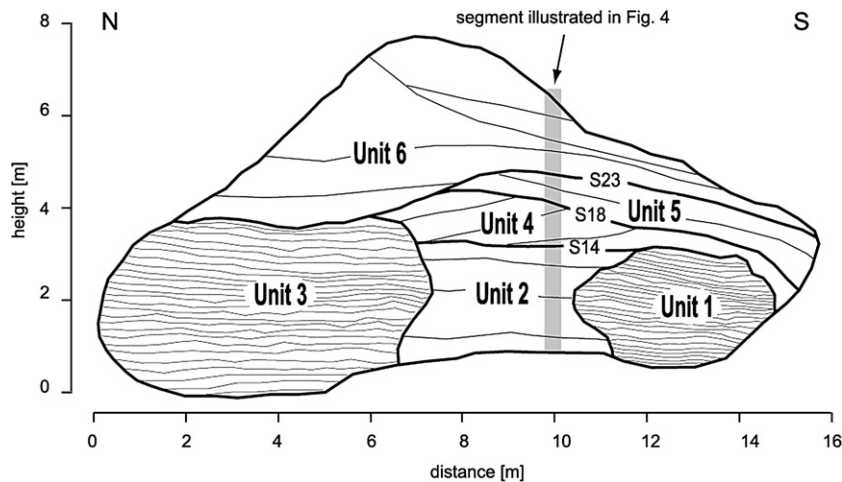


Figure 3. Schematized ice sequence observed in the St. Livres ice cave with the six stratigraphic units. Layers *S14*, *S18* and *S23* represent major stratigraphic unconformities underlined by organic detrital material. The gray surface indicates the position of the stratigraphic log represented in Figure 4.

| Depth | Unit | Layer | Stratigraphy | Lithology | Tree-ring samples | ¹⁴ C samples |
|-------|--------|-------|--------------|--|---|-------------------------|
| 0 m | Unit 6 | 27 | | ice surface: cryoclasts, anthropogenic material, leaves, branches and older trunks | StL-76; StL-77; StL-78; StL-80 StL-82 | |
| -1 m | | 23 | | trunk, branches (<i>Picea abies</i>), plank (#45) | StL-44; StL-47; StL-49 | |
| -2 m | Unit 5 | | | bones (<i>Sus scrofa domestica</i>), trunk (<i>Picea abies</i>) | StL-29; StL-56 | |
| -2 m | | | | beam, branches (<i>Picea abies</i>) | StL-17, StL-18 StL-55; StL-57; StL-58; StL-81 | ETH 29536 |
| -3 m | Unit 4 | 18 | | bones (<i>Sus scrofa domestica</i>), trunk (<i>Picea abies</i>), leaves (<i>Fagus sylvatica</i>) | StL-01; StL-05; StL-10; StL-28; StL-43 StL-75 | |
| -3 m | | | | cryoclasts, plank, twigs, cones (<i>Picea abies</i>) | StL-23; StL-25; StL-31; StL-33 | |
| -4 m | Unit 2 | | | plank, leaves (<i>Fagus sylvatica</i>) | | |
| -4 m | | 14 | | isolated trunk cryoclasts (dm), trunc, twigs (<i>Picea abies</i>) plank | StL-32; StL-37; StL-42; StL-50; StL-62; StL-71; StL-72; StL-73 | ETH 29535 |
| -5 m | Unit 2 | | | moss, occasional cryoclasts | | |
| -5 m | | 10 | | cryoclasts (cm), cones (<i>Picea abies</i>), moss detrital organic material cryoclasts (cm) | | |
| -6 m | Unit 2 | | | branches, twigs | | |
| -6 m | | 5 | | cryoclasts (cm), twigs, cones (<i>Picea abies</i>) | | ETH 29534 |
| -6 m | | 1 | | remobilized trunk | | ETH 28592 |

Figure 4. Stratigraphic log of the central part of the St. Livres cave-ice deposit with details on the lithology and the position of *P. abies* trunks and branches used for dendrochronological analyses and radiocarbon dating.

Unit 4 is overlapping the erosive layer *S14* and shows an angular discordance with the underlying stratigraphic *Units 1* and *2*. This unit consists of firm deposits and contains three major organic layers (*S15–S17*) being in good stratigraphic conformity. Large stems are observed displaying a mean dip of 60°, which is in good agreement with the general slope of the cave-ice accumulation. The top of *Unit 4* is again truncated by an erosive contact underlined by the organic layer *S18*.

The base of *Unit 5* is delineated by an erosive contact that can be observed along the entire ice front, truncating *Units 1, 3* and *4*, respectively. The contact is underlined by a ~10 cm thick layer rich in organic material (*S18*) such as trunks, branches, leaves, several bones from a domestic pig (*Sus scrofa domestica*, M. Blant, SSKA, *verbatim*) and soil litter. Generally, the unit consists of anisotropic firm deposits, interlayered by centimetric strata rich in organic material. Anthropogenic material is observed in the form of planks and pieces of beams from a ladder containing post-industrial nails (D. Weidmann, state archaeologist, *verbatim*).

The base of *Unit 6* is delineated by an erosive contact, merging with layer *S18* on the northern part of the outcrop. This unit consists mainly of cross-stratified firm accumulations interlayered with organic deposits, comprising trunks, branches and leaves from the exterior vegetation as well as soil litter material. Some of the clastic elements observed in this unit show an anthropogenic origin such as nails and cut branches.

Dendrochronological dating of subfossil trees

A statistical comparison of the local (“St. Livres”) with the regional (“Jura”) tree-ring chronologies was achieved for the period 1789–1986. The chronologies show parallelisms (*Glk*) of 66; a cross-date index (*CDI*) 217 and a Cofecha correlation (*p*) of 0.46 (see Fig. 5).

Consequently, both series were used for the dating of the cave-ice cross-sections, thus allowing reconstruction of outer-ring ages for 34

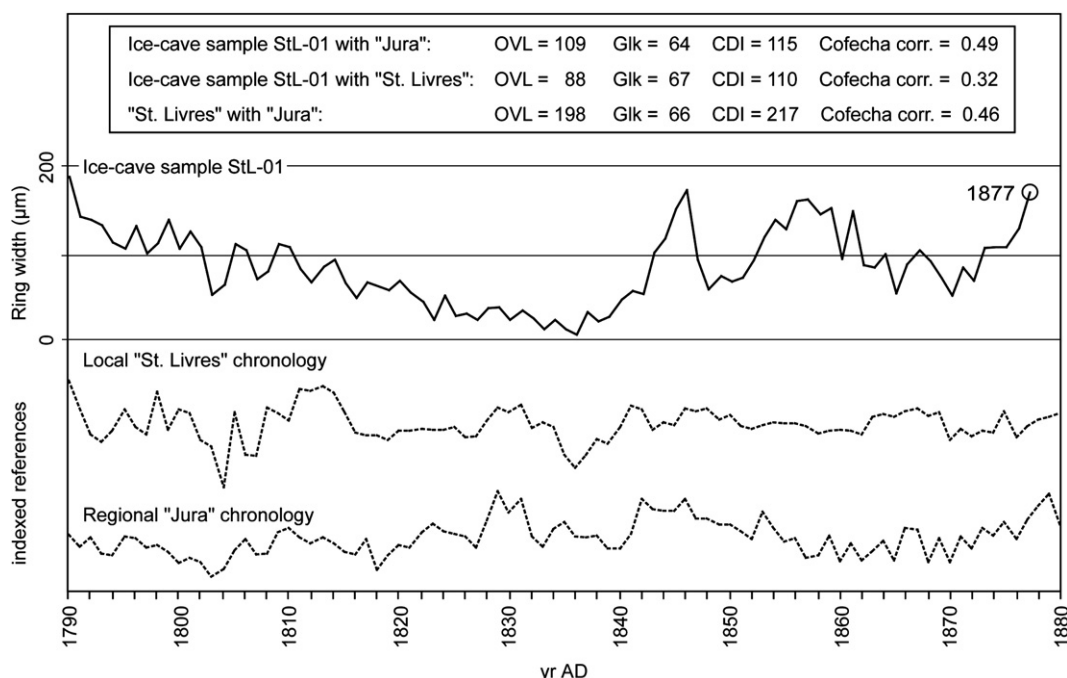


Figure 5. Dendrochronological cross-dating of ice-cave sample StL-01 with the local (“St. Livres”) and the regional (“Jura”) chronologies. Details on the cross-dating values between the undated wood sample and the chronologies as well as the values between the two series can be found in the main text.

of the 45 *P. abies* samples. Five of the dated ice-cave samples show signs of wood processing and presumably served as rungs so as to facilitate cave access. Eleven ice-cave samples did neither fulfill the criteria listed above nor could they be cross-dated with the local (“St. Livres”) or the regional (“Jura”) tree-ring chronologies.

According to the results of the cross-dating, outermost rings of the wood samples were dated to the period AD 1305–1956, with a majority of trees showing last rings in the second half of the 19th century. Dendrochronological data show an increasing age of subfossil trees with depth. The oldest datable samples are located in the organic layers of Unit 4 (S15), where eight samples show outer-ring ages between AD 1305–1393. In layer S17, five *P. abies* samples were dated to AD 1415–1478. In the firm deposits between layers S17 and S18, a piece of processed wood (plank) was analyzed and dated to AD 1688.

Two trunks were sampled from the organic layer S18 (i.e., the erosive contact between Units 4 and 5), one showing an outermost ring in 1857, the other one in 1861. In the overlaying Unit 5, tree-ring analysis allowed dating of nine trunks and branches belonging to

three distinct organic layers. We obtain outer-ring ages located in the 1870s for S20, 1880s for S21 and AD 1891 for the two samples originating from uppermost organic layer of Unit 5 (S23).

Samples from Unit 6 were taken at the erosive contact with Unit 5 (S23) and from the current-day ice surface. Three dated samples from this contact layer show outer-ring ages between AD 1898 and 1900. Four trunks were sampled on the current-day ice surface close to the ice front and one cross-section taken from a *P. abies* laying on the surface of the ice body below the entrance shaft. All these samples were no longer in their original position, reason why outer-ring ages largely varied from AD 1832 to 1908 close to the ice front. The last tree ring of the trunk located below the entrance shaft was formed in AD 1956.

Radiocarbon dates of subfossil trees and organic material

Results of the radiocarbon dating are shown in Table 1 and display an increasing age with depth. For the samples selected at the bottom of the cave-ice deposit (i.e., layers S1 and S4), a maximal age of about

Table 1
Radiocarbon (¹⁴C) datings of organic material from the St. Livres ice cave.

| Sample no | Stratigraphic unit | Layer | Stratigraphic depth (m) | AMS- ¹⁴ C age [¹⁴ C yr BP] | δ ¹³ C [‰] | Calibrated age [AD] | 2σ-confidence (%) |
|------------------|--------------------|-------|-------------------------|--|--------------------------|--|----------------------------------|
| ETH-29536 | Unit 5 | 20 | −1.7 | 190 ± 45 ¹⁴ C yr BP | −25.1 ± 1.2 | AD 1643–1707 AD 1719–1821 AD 1827–1884 AD 1913–1950 | 23.80 50.50 10.20 15.50 |
| ETH-29535 | Unit 4 | 14 | −3.6 | 1040 ± 50 ¹⁴ C yr BP | −25.5 ± 1.2 | AD 890–1056 AD 1088–1122 | 90.60 5.80 |
| ETH-30880 | Unit 1 | | −4.2 | 1030 ± 45 ¹⁴ C yr BP | −24.7 ± 1.1 | AD 894–924 AD 936–1056 AD 1088–1122 AD 1138–1156 | 9.80 78.50 7.10 4.60 |
| ETH-29534 | Unit 2 | 5 | −5.2 | 1200 ± 50 ¹⁴ C yr BP | −25.6 ± 1.2 | AD 706–754 AD 757–903 AD 916–963 | 12.20 74.10 11.00 |
| ETH-28592 | Unit 2 | 1 | −5.7 | 970 ± 45 ¹⁴ C yr BP | −24.6 ± 1.2 | AD 990–1163 AD 1172–1184 | 98.10 1.90 |
| ETH-30881 | Unit 3 | | −4.6 | 960 ± 45 ¹⁴ C yr BP | −22.8 ± 1.1 | AD 998–1164 AD 1169–1187 | 96.50 3.50 |

The bold emphasis refers to samples shown in the stratigraphic log of Fig. 4.

1200 yr is suggested. It is also worthwhile to note that for the samples analyzed in the upper units (S14, S20), radiocarbon data are in very good agreement with the outer-ring ages from the dendrochronological analysis.

Cave-ice chronostratigraphy – a synthesis

Dendrochronological analysis of 34 subfossil wood samples and radiocarbon dating of six samples of associated organic material identified several periods of intermittent ice accumulation in St. Livres cave. Figure 6 summarizes these results in an age model together with the cave-ice stratigraphy. A consistent increase in age is observed with depth although a large scattering of the data is noticed in the most recent layer. Five samples selected from the present-day ice surface (StL-76; StL-77; StL-78; StL-80 and StL-82) show outer-ring ages ranging from AD 1832–1956 (Table 2). These data suggest that the large amount of organic material observed on the current-day ice surface corresponds to a concentration of various organic rich layers following recent cave-ice ablation.

From the ice-cave stratigraphy and based on the results of dendrochronological dating, we identify four additional major ablation events leading to negative cave-ice mass balances. Figure 6 also points to a period of intermittent cave-ice accumulation (Unit 5) lasting from 1826 to 1898, interrupted by three individual detrital layers underlining short periods of cave-ice ablation (S20, S21 and S22). These layers have been tree-ring dated with eight cross-sections (samples StL-17; StL-18; StL-29; StL-55; StL-56; StL-57; StL-58; and StL-81) to the period 1877–1878, 1883–1884, and 1891, respectively. From the dating of nine subfossil wood samples extracted from layers S18 to S20 we also identify a period of higher cave-ice accumulation rates between 1826 to 1877 (samples StL-1; StL-5; StL-10; StL-28; StL-43; StL-55; StL-57; StL-58 and StL-81).

Another period with large amounts of organic clasts comprises layer S17, where four cross-sections (samples StL-23, StL-25, StL-31 and StL-33) indicate the existence of an important accumulation gap over the 15th century, with outer-ring ages of samples ranging between 1415 and 1531. From our data, we also identify a period of

negative cave-ice mass balance represented by organic layer S15. Based on the cross-dating results of eight cross-sections (samples StL-32; StL-37; StL-42; StL-50; StL-62; StL-71; StL-72 and StL-73), we are able to date this accumulation gap to the 14th century (1305–1393).

The oldest truncating layer (S14) was out of range of the dendrochronological reference curve and has therefore been assessed with radiocarbon analyses to 1040 ± 50 ^{14}C yr BP (ETH-29535). Based on field observations, it appears that this period with negative cave-ice mass balance has led to the formation of the erosive contact truncating the top of stratigraphical Units 1 and 2 (see Figs. 3 and 4). From the ^{14}C data, we also suggest that cave-ice deposition rates were significantly higher during the deposition of stratigraphical Unit 2 ranging between 1200 ± 50 ^{14}C yr BP (ETH-29534) and the ablation event at 1040 ± 50 ^{14}C yr BP (ETH-29535).

Discussion

This study reports the use of dendrochronological and radiocarbon methods to date the ice sequence of the low-elevation St. Livres ice cave in the Jura Mountains (Switzerland) from 45 subfossil *P. abies* (L.) Karst. wood samples as well as seven radiocarbon (^{14}C) datings from wood pieces and organic litter buried in the 8 m thick cave-ice stratigraphy. Results suggest a maximal age for the observed ice sequence of 1200 ± 50 ^{14}C yr BP (ETH-29534), indicating that subsurface cave ice would have been continuously present in the Jura Mountains for at least the last 1200 yr. This finding is unique for non-glaciated areas of the European Alps and most relevant for a process-based understanding of sporadic permafrost occurrences at low-elevation sites as well as for investigations of Holocene permafrost changes. Data also indicate that at least four major deposition gaps occurred between 1200 ± 50 ^{14}C yr BP and today.

Dendrochronological dating of the buried *P. abies* trunks and branches yielded statistically sound and reliable calendar dates in 34 cases (78%). In contrast, dating was not possible for eleven cross-sections (22%): in seven cases, cave-ice samples had <28 increment rings and were typically branches or pieces of processed wood. The tree-ring series measured from these samples were considered too short for

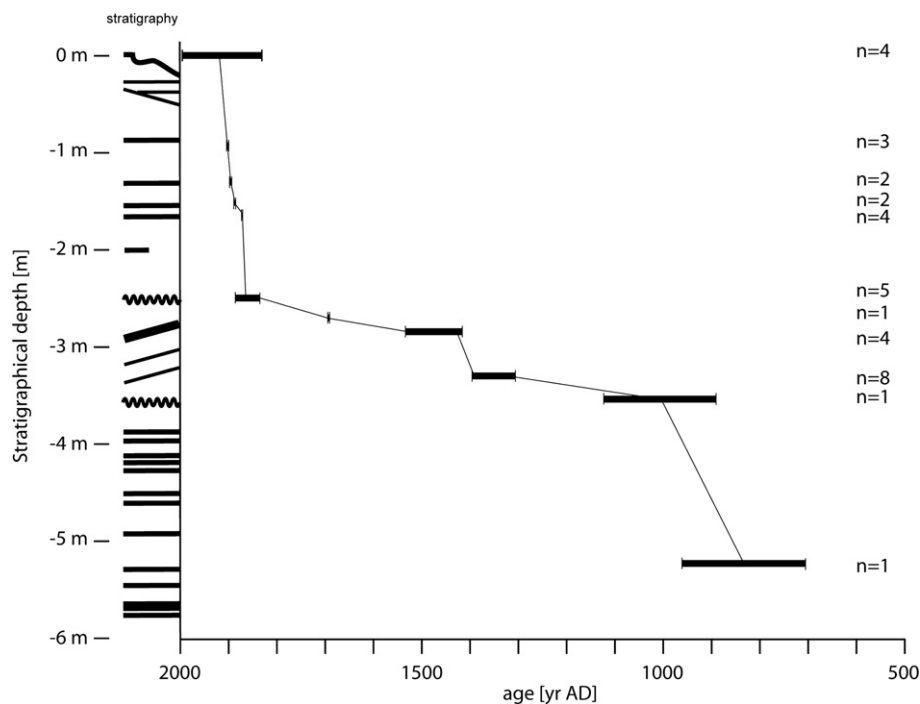


Figure 6. Age model of ice deposition in St. Livres cave shown together with the cave-ice stratigraphy. Number of dated samples per strata is given on the right. The linear interpolation follows a best estimate of cave-ice accumulation phases as determined by the dating of organic detrital material.

Table 2

Dendrochronological dates of subfossil tree samples enclosed in the St-Livres cave-ice sequence.

| Unit | Detrital layer | Sample no. | Tree-ring sequence (number of rings) | Presence of bark | Overlap (yr) | Reference(s) used (St. Livres; Jura) | Outermost ring (yr AD) | Quality |
|------|----------------|------------|--------------------------------------|------------------|--------------|--------------------------------------|------------------------|---------|
| 6 | 27 | StL-82 | 144 | Yes | 144 | St. Livres, Jura | 1956 | *** |
| 6 | 27 | StL-80 | 105 | No | 105 | St. Livres, Jura | 1908 | *** |
| 6 | 27 | StL-76 | 58 | Yes | 58 | St. Livres, Jura | 1853 | *** |
| 6 | 27 | StL-78 | 37 | Yes | 37 | Jura | 1834 | ** |
| 6 | 27 | StL-77 | 39 | Yes | 39 | St. Livres | 1832 | ** |
| 6 | 23 | StL-49 | 61 | Yes | 61 | St. Livres, Jura | 1900 | *** |
| 6 | 23 | StL-47 | 80 | Yes | 80 | St. Livres | 1899 | ** |
| 6 | 23 | StL-44 | 50 | No | 50 | St. Livres, Jura | 1898 | *** |
| 5 | 22 | StL-29 | 100 | No | 100 | St. Livres | 1891 | * |
| 5 | 22 | StL-56 | 44 | Yes | 44 | St. Livres, Jura | 1891 | *** |
| 5 | 21 | StL-18 | 45 | Yes | 45 | St. Livres, Jura | 1884 | *** |
| 5 | 21 | StL-17 | 63 | Yes | 63 | St. Livres | 1883 | ** |
| 5 | 20 | StL-58 | 28 | Yes | 28 | St. Livres, Jura | 1878 | * |
| 5 | 20 | StL-55 | 42 | No | 42 | St. Livres, Jura | 1877 | *** |
| 5 | 20 | StL-57 | 28 | No | 28 | St. Livres, Jura | 1877 | ** |
| 5 | 20 | StL-81 | 96 | Yes | 96 | St. Livres | 1877 | ** |
| 5 | 18 | StL-01 | 109 | No | 109 | St. Livres, Jura | 1877 | *** |
| 5 | 18 | StL-28 | 41 | Yes | 41 | St. Livres | 1861 | ** |
| 5 | 18 | StL-05 | 61 | No | 61 | St. Livres, Jura | 1858 | *** |
| 5 | 18 | StL-43 | 81 | Yes | 81 | St. Livres, Jura | 1857 | ** |
| 5 | 18 | StL-10 | 71 | Yes | 37 | St. Livres | 1826 | ** |
| 4 | | StL-75 | 42 | No | 42 | Jura | 1688 | *** |
| 4 | 17 | StL-33 | 46 | No | 46 | Jura | 1531 | * |
| 4 | 17 | StL-31 | 77 | Yes | 77 | Jura | 1478 | *** |
| 4 | 17 | StL-25 | 32 | Yes | 32 | Jura | 1446 | ** |
| 4 | 17 | StL-23 | 34 | No | 34 | Jura | 1415 | ** |
| 4 | 15 | StL-32 | 69 | No | 69 | Jura | 1393 | *** |
| 4 | 15 | StL-72 | 73 | Yes | 73 | Jura | 1384 | ** |
| 4 | 15 | StL-71 | 46 | No | 46 | Jura | 1377 | * |
| 4 | 15 | StL-50 | 35 | No | 35 | Jura | 1376 | ** |
| 4 | 15 | StL-37 | 50 | No | 50 | Jura | 1355 | *** |
| 4 | 15 | StL-42 | 51 | Yes | 51 | Jura | 1320 | ** |
| 4 | 15 | StL-73 | 32 | Yes | 32 | Jura | 1312 | * |
| 4 | 15 | StL-62 | 44 | Yes | 44 | Jura | 1305 | * |

The quality of reconstructed outer-ring ages was based on: (i) length of the tree-ring series; (ii) maximum overlap between the series of the subfossil sample and the chronologies; (iii) parallelism (Glk) between the subfossil sample series and the reference chronologies; (iv) cross-date index; (v) Cofecha correlation value; (vi) results confirmed by both chronologies for samples with an inner-ring age younger than AD 1789. For details, see text.

accurate dating. In addition, a comparison of buried samples with the reference chronologies did not yield results at all for four cross-sections. Based on its position at the bottom of the stratigraphy, it seems likely that one of the samples was simply too old for dendrochronological cross-dating. In contrast, the three other samples were located in layers that have been dated with other trees (i.e. current ice surface and organic layer S15), but their degree of decomposition was such that the quality of the wood was the limiting factor for the dating.

It is worthwhile to notice that high correlation values between different *P. abies* samples or even chronologies are not easily achieved, as the species show complacent growth which is driven by site-specific rather than regional conditions (*P. Gassmann*, state dendroarcheologist, *verbatim*). Another element to be considered in the dating of the ice-cave samples is that the trees were standing on the steep slopes of the cave entrance and were repeatedly influenced by different geomorphic processes. The subsequent tilting of stems, the exposure of roots and various kinds of mechanical stress (e.g., wind, snow, or rockfall) have sometimes resulted in abnormal tree-ring growth (e.g., eccentric growth, abrupt growth decrease, tangential rows of traumatic resin ducts; see *Bollschweiler et al., 2008; Stoffel and Bollschweiler, 2008; Stoffel et al., 2008*), which may also influence the quality of growth concordance between the cave-ice samples on one hand and the local or regional chronologies on the other hand.

Other elements to be taken into account are the (i) time elapsed between the death of the tree and its actual fall into the cave as well as (ii) the residence time of samples on the cave ice before burial. Empirical data on the time elapsed between the death of a *P. abies* tree and its actual fall are inexistent for steep slopes. *Storaunet and Rolstad (2002, 2004)* suggest median standing times of 16–21 yr for *P. abies* snags in Fennoscandian forests. While the St. Livres site is characterized by comparable total annual precipitation and mean annual

temperature, it completely differs from the Fennoscandian sites in terms of geomorphology (steep slopes vs. flat terrain) and snowload characteristics (dense-wet snow versus light-dry snow). Based on these considerations, we believe that standing times of deadwood around the entrance of the St. Livres cave are considerably lower than in the forests analyzed by *Storaunet and Rolstad (2002, 2004)* and that *P. abies* trees at St. Livres fell down onto the cave-ice deposits shortly after their death due to the steep slope and/or snowload in winter. It seems also that some of the cave-ice trees were buried with their root collar and probably overthrown by (winter) storms.

The limited degree of decomposition of *P. abies* samples (i.e. conservation of bark and twigs) suggests that comparably little time has elapsed between the death of the trees and their actual fall onto the ice deposit (*McCullough, 1948; Söderström, 1988; Hofgaard, 1993*). Even though decay processes are retarded in the cold environment of the ice cave, the good state of conservation of most cross-sections also indicates that the residence time of samples on the cave ice before burial is not too important either.

Despite the above limitations of the approach, dendrochronology remains by far the most reliable method for the dating of organic material buried in ice caves, provided that there is a sufficient amount of tree-rings (>28 yr) available. Conversely to radiocarbon dating, the uncertainty is reduced to the time elapsed between the death of the tree, its actual fall into the cave and the burial inside the cave-ice body. Dendrochronological approaches are normally based on a local reference curve that entirely covers the investigated time window of subfossil samples. As *P. abies* rarely gets older than 200 yr (*Ott et al., 1997*) and due to the lack of historical proxies in the surrounding area (e.g., old beams), a supra-regional reference curve built with *P. abies* and *A. alba* Mill. (see *Gassmann, 2007*) was used for the cross-dating of older cave-ice samples. The results issued from the successful dating of 34

wood samples extracted from the St. Livres ice cave and the good agreement between the local and the regional chronologies justify the use of a supra-regional reference curve and provide a valuable chronostratigraphic framework for further paleoenvironmental studies.

The wood samples analyzed from St. Livres ice cave were collected from eight distinct organic rich layers outcropping at the ice front. The individually dated strata are attributed to major phases of cave-ice ablation, concentrating several years of detrital material deposition. The large scattering of data observed in some of the strata (for instance, layer *S15*: AD 1305–1393, $n = 8$) suggests that detrital rich layers delineating major sedimentation units may sometimes represent several decades of negative cave-ice mass balance. This interpretation is also consistent with the dating of 170 yr old samples from the modern ice surface.

Recent studies based on modern surveys of cave-ice fluctuations suggested that cave-ice mass balances mainly reflect temperature and precipitation regime during the winter season (e.g. Ohata et al., 1994a,b; Luetscher et al., 2005). Net cave-ice accumulation is therefore preferentially achieved during cold winters experiencing large snow precipitations. In contrast, warm and humid summers contribute to the seasonal ablation of the cave-ice surface, thus favoring negative mass balances with seasonal ablation rates exceeding the annual cave-ice formation.

From our data, we identified four major accumulation gaps during the 20th century, the 19th century (AD 1826–1877), the 15th century (AD 1415–1531) and the 14th century (AD 1305–1393) respectively. In contrast, major cave-ice accumulation is observed during the 19th and early 20th century (*Unit 5* and *6*). Comparison with homogenized regional meteorological data (Begert et al., 2005) confirms the climate dependency of the cave-ice mass balance. Low winter temperatures (1885–1891) associated with large snow precipitation (1886–1888) may explain the approximately 25 cm thick firn layer dated between 1884 and 1891. Wet and cold winter conditions experienced in 1876 are also likely to explain the positive cave-ice mass balance documented just before 1877 (i.e. layer *S20*). Conversely, warm and dry winters followed by increased precipitation during the summer season may explain the negative cave-ice mass balance associated with the organic rich layer *S20*.

Historical records of regional paleoclimatic patterns and anomalies are scarce but a supra-regional chronology of temperature and precipitation variations as well as data on winter NAO indices are available since AD 1496 and AD 1400, respectively (Pfister 1999; Cook et al., 2002). A comparison with these paleoclimatic records reveals that there is strong evidence for major periods of cave-ice accumulation and ablation at St. Livres ice cave being closely related to winter North Atlantic Oscillation (NAO) indices (Cook et al., 2002). According to these data, the period between 1520 and 1545 was marked by a positive winter NAO index (Cook et al., 2002) in general and warm and dry winter climate anomalies in Switzerland in particular (Pfister, 1999), which could have led to abundant cave-ice ablation over almost three decades and produce the “AD 1415–1531” accumulation gap underlined by the organic deposits of layer *S17*. Considering the area is likely to have experienced more abundant summer precipitation during the same period (e.g., Casty et al., 2005; Magny et al., 2008), we argue that this organic rich detrital layer in St. Livres ice cave may clearly reflect a climatic signal.

Based on our data, we believe that another period of positive winter NAO indices prevailed during the late 14th century, which would have produced the “AD 1305–1393” ablation identified in the cave-ice chronostratigraphy at St. Livres. Radiocarbon dates from layer *S14* indicate the presence of yet another ablation event around 1040 ± 50 ^{14}C yr BP, but the low resolution of the methods used hinders a more precise dating of these undocumented periods of presumably positive winter NAO anomalies.

In contradiction with existing climate proxies suggesting cool and wet winter conditions during the 19th century, data from St. Livres ice cave also show that a marked phase of ablation occurred during the same period (layer *S18*: AD 1826–1877). The presence of

numerous anthropogenic clasts from stratigraphical *Unit 5* upwards suggests however that this ablation has an anthropogenic rather than a natural origin. This assumption is supported further by historical documents describing the presence of local cave-ice abstraction from St. Livres ice cave during the 19th century. According to Browne (1865) this abstraction lasted several decades and represented nearly 50 m³ in AD 1863. Although little information is available for older periods it is likely that cave-ice abstraction started during the 17th century already when the regional pasture expansion reached a paroxysm (Sjögren, 2006). This interpretation is also in good agreement with the presence of a plank dated to 1688 in the upper part of *Unit 4* (StL-75).

While it may be difficult to extract a precise timing of enhanced ablation phases, organic rich layers offer the potential to delineate accurately periods of cave-ice accumulation. Such a period of natural cave-ice accumulation is identified between AD 1877 and 1900, when a negative winter NAO index (Cook et al., 2002) and cool and wet conditions (Pfister, 1999) have favored a positive ice-cave mass balance. Based on our records, there is evidence for another accumulation phase during AD 1393–1415. During these years at the end of 14th and the early 15th century, Cook et al. (2002) note a negative winter NAO index. Our radiocarbon data suggest that the St. Livres ice cave experienced comparably high cave-ice accumulation rates between approximately AD 706 and AD 1156 (2σ range). Our data are in good agreement with evidence of mild winter temperatures in the Central Alps centered around AD 1000 (Mangini et al., 2005) possibly associated with persistent westerly airflow patterns (Bradley et al., 2003) leading to increased snow precipitation in the Jura Mountains and the absence of major ice-ablation events resulting from positive winter NAO indices.

While there is little chronological evidence for the initiation of ice accumulation in St. Livres cave, our data reveal a less dynamic system than for instance in Monlési ice cave (Luetscher et al., 2007). This reduced mass turnover rate is attributed to local ventilation patterns in the scree slope underneath the cave-ice volume, limiting heat exchanges with the surrounding karst system (Luetscher et al., 2008). The latter might be an indication of cold basal ice layers favorable for the preservation of a local isotopic record of winter precipitation.

Conclusions

Establishing a sound chronology for the ice sequences observed in caves of the Jura Mountains is an essential step for the realization of detailed paleoenvironmental studies at these climatically sensitive sites. Our data also shows that cave-ice accumulation at St. Livres is closely related to winter NAO and that cave ice represents therefore an original and valuable climate archive for the winter half-year and has to be seen complementary to other continental proxies which record preferentially summer conditions (e.g., tree-rings, varves). Although the accessible time window at St. Livres ice cave covers over 1200 yr, our study demonstrated the presence of a discontinuous accumulation sequence, which would need a detailed three dimensional stratigraphic analysis to be deciphered. Continuous ice-core studies, as recommended by Citterio et al. (2004), are, in contrast, probably not relevant for this study site. But, the presence of thousand year old frozen organic material identified in the individually dated layers could potentially contribute to the reconstruction of regional vegetation changes (van der Knaap et al., 2005). This issue gains particular interest as deforestation of the current pastures apparently took place during the 12th and 13th centuries.

Results obtained for the different ice layers at St. Livres cave represent one of the most detailed analyses of this kind. In contrast to ice caves where results are often based on unique samples and only a rather limited amount of organic material, the large number of buried trunks and branches present in the St. Livres ice cave enabled reconstruction of a detailed cave-ice chronostratigraphy.

Our data represent a unique and original archive of cave-ice accumulation and ablation periods in the Jura Mountains, where similar records were missing so far. This study also contributes to a better understanding of the regional precipitation regime and NAO indices during the winter half-year extending available proxies to the Medieval Warm Period, lasting approximately from about AD 800 to AD 1300. Despite the difficulty of extracting a continuous record from this archive, the methodology presented here represents an innovative way of dating subsurface ice deposits. Further studies will allow assessing in more details the potential of cave ice for detailed paleoenvironmental studies in non-glaciated areas.

Acknowledgments

This study would not have been possible without the support of Dr. Patrick Gassmann, Laboratory of Dendrochronology, Laténium-Neuchâtel, who provided the regional reference curve. We also acknowledge Dominique M. Schneuwly for the analysis of some of the subfossil cross-sections. This work has been supported by the Swiss National Science Foundation (project No. 21-63764.00 and No. PBZH2-112727), whereas the Fonds du Centenaire of the University of Fribourg (grant No 255) has sponsored some of the ^{14}C and dendrochronological datings. We also thank Alan Gillespie, Michael A. O'Neal and two anonymous referees for their careful reviews that prompted substantial improvements in this paper.

References

- Aubert, D., 1969. Phénomènes et formes du Karst jurassien. *Eclogae geologicae Helvetiae* 62, 325–399.
- Audétat, M., Heiss, G., Christen, D., Deriaz, P., Heiss, C., Luetscher, M., Morel, P., Perrin, J., Wittwer, M., 2002. Inventaire spéléologique du Jura vaudois, partie ouest. Commission spéléologique de l'Académie Suisse des Sciences Naturelles, La Chaux-de-Fonds. 536 pp.
- Begert, M., Schlegel, T., Kirchhofer, W., 2005. Homogeneous temperature and precipitation series of Switzerland from 1864–2000. *International Journal of Climatologia* 25, 65–80.
- Buttler, A., Gillet, F., Gobat, J.M., 2001. Végétation et flore. In: Blant, M. (Ed.), *Le Jura: les paysages, la vie sauvage, les terroirs*. Delachaux et Niestlé, Paris, pp. 77–151.
- Bollschweiler, M., Stoffel, M., Schneuwly, D.M., Bourqui, K., 2008. Traumatic resin ducts in *Larix decidua* trees impacted by debris flows. *Tree Physiology* 28, 255–263.
- Bradley, R.S., Hughes, M.K., Diaz, H.F., 2003. Climate in Medieval time. *Science* 302, 404–405.
- Bräker, O.U., 2002. Measuring and data processing in tree-ring research – a methodological introduction. *Dendrochronologia* 20 (1–2), 203–216.
- Browne, G.F., 1865. Ice Caves of France and Switzerland: a Narration of Subterranean Exploration. Longmans Green, London.
- Casty, C., Wanner, H., Luterbacher, J., Esper, J., Boehm, R., 2005. Temperature and precipitation variability in the European Alps since AD 1500. *International Journal of Climatologia* 25, 1855–1880.
- Cecil, L.D., Green, J.R., Thompson, L.G. (Eds.), 2004. *Earth Paleoenvironments: Records Preserved in Mid- and Low Altitude Glaciers*. Developments in Paleoenvironmental Research. Kluwer Academic Publishers, p. 250.
- Citterio, M., Turri, S., Bini, A., Maggi, V., Pini, R., Ravazzi, C., Santilli, M., Stenni, B., Udisti, R., 2004. Multidisciplinary approach to the study of the Lo Lc 1650 "Abisso sul Margine dell'Alto Bregai" ice cave (Lecco, Italy). *Theoretical and Applied Karstology* 17, 45–50.
- Clausen, H.B., Vrana, K., Hansen, S.B., Larsen, L.B., Baker, J., Siggaard-Andersen, M.L., Sjolte, J., Lundholm, S.C., 2007. Continental ice body in Dobsina Ice Cave (Slovakia) – Part II. – Results of chemical and isotopic study. In: Zelinka, J. (Ed.), *Proceedings of the 2nd International Workshop on Ice Caves, IWIC-II, Demanovska Dolina, Slovak Republic*, pp. 29–37.
- Cook, E.R., Kairiukstis, L., 1990. *Methods of Dendrochronology. Applications in the Environmental Sciences*. Kluwer, Dordrecht.
- Cook, E.R., D'Arrigo, R.D., Mann, M.E., 2002. A well-verified, multiproxy reconstruction of the winter North Atlantic Oscillation index since A.D. 1400. *Journal of Climate* 15, 1754–1764.
- Eckstein, D., Bauch, J., 1969. Beitrag zur Rationalisierung eines dendrochronologischen Verfahrens und zur Analyse seiner Aussagesicherheit. *Forstwissenschaftliches Centralblatt* 88, 230–250.
- Egger, H., Gassmann, P., Burri, N., 1985. Situation actuelle du travail au laboratoire de dendrochronologie de Neuchâtel. *Dendrochronologia* 3, 177–192.
- Gassmann, P., 2007. *Picea abies* (L.) Karst. and *Abies alba* Mill. chronology of the Neuchâtel Jura 1200–1986. Neuchâtel Archeology Service, Laténium (unpublished data).
- Grissino-Mayer, H.D., 2001. Evaluating crossdating accuracy: a manual and tutorial for the computer program COFECHA. *Tree-Ring Research* 57, 205–221.
- Haeblerli, W., Frauenfelder, R., Käab, A., Wagner, S., 2004. Characteristics and potential climatic significance of "miniature ice caps" (crest-and cornice-type low-altitude ice archives). *Journal of Glaciology* 50, 129–136.
- Hofgaard, A., 1993. Structure and regeneration patterns in a virgin *Picea abies* forest in northern Sweden. *Journal of Vegetation Science* 4, 601–608.
- Holmes, R.L., 1983. Computer assisted quality control in tree-ring dating and measurement. *Tree-Ring Bulletin* 43, 69–78.
- Holmlund, P., Onac, B.P., Hansson, M., Holmgren, K., Mörth, M., Nyman, M., Persoiu, A., 2005. Assessing the paleoclimate potential of cave glaciers: the example of the Scarisoara ice cave (Romania). *Geografiska Annaler* 87A 193–201.
- Keller, F., Frauenfelder, R., Hoelzle, M., Kneisel, C., Lugon, R., Phillips, M., Reynard, E., Wenker, L., 1998. Permafrost map of Switzerland. *Collection Nordica. Centre d'Études Nordiques, Université Laval* 57, 557–568.
- Kern, Z., Molnar, M., Persoiu, A., Nagy, B., 2007. Radiochemical and stratigraphic analysis of two ice cores from Bortig Ice Cave, Apuseni Mts, Romania. In: Zelinka, J. (Ed.), *Proceedings of the 2nd International Workshop on ice caves, IWIC-II, Demanovska Dolina, Slovak Republic*, pp. 65–69.
- Luetscher, M., Lismonde, B., Jeannin, P.Y., 2008. Heat exchanges in the heterothermic zone of a karst system: Monlesi cave, Swiss Jura Mountains. *Journal of Geophysical Research* 113, F02025.
- Luetscher, M., Bolius, D., Schwikowski, M., Schotterer, U., Smart, P.L., 2007. Comparison of techniques for dating of subsurface ice from Monlesi ice cave, Switzerland. *Journal of Glaciology* 53, 374–384.
- Luetscher, M., Jeannin, P.Y., Haeblerli, W., 2005. Ice caves as an indicator of winter climate evolution—a case study from the Jura Mountains. *The Holocene* 15, 982–993.
- Magny, M., Gauthier, E., Vannière, B., Peyron, O., 2008. Palaeohydrological changes and human-impact history over the last millennium recorded at Lake Joux in the Jura Mountains, Switzerland. *Holocene* 18 (2), 255–265.
- Mangini, A., Spötl, C., Verdes, P., 2005. Reconstruction of temperature in the Central Alps during the past 2000 yr from a $\delta^{18}\text{O}$ stalagmite record. *Earth and Planetary Science Letters* 235, 741–751.
- McCullough, H., 1948. Plant succession on fallen logs in a virgin spruce-fir forest. *Ecology* 29, 508–513.
- MeteoSwiss, 2008. <http://www.meteoschweiz.admin.ch/web/en/weather.html> (site consulted on July 11, 2008)
- Niklaus, T.R., Bonani, G., Simonius, M., Suter, M., Wölfli, W., 1992. CalibETH: an interactive computer program for the calibration of radiocarbon dates. *Radiocarbon* 34 (3), 483–492.
- Ohata, T., Furukawa, T., Higuchi, K., 1994a. Glacioclimatological study of perennial ice in the Fuji ice cave, Japan. 1. Seasonal variation and mechanism of maintenance. *Arctic and Alpine Research* 26, 227–237.
- Ohata, T., Furukawa, T., Osada, K., 1994b. Glacioclimatological study of perennial ice in the Fuji ice cave, Japan. 2. Interannual variation and relation to climate. *Arctic and Alpine Research* 26, 238–244.
- Ott, E., Frehner, M., Frey, H.U., Lüscher, P., 1997. *Gebirgsnadelwälder: Ein praxisorientierter Leitfaden für eine standortgerechte Waldbehandlung*. Paul Haupt, Bern, Stuttgart, Wien.
- Pfister, C., 1999. *Wetternachhersage. 500 Jahre Klimavariationen und Naturkatastrophen*. Paul Haupt Verlag, Bern, Stuttgart, Wien.
- Rinn, F., 1989. *Time Series Analysis and Presentation V3.0. Reference Manual*. Rinntech, Heidelberg.
- Rinntech, 2008. <http://www.rinntech.com/Products/Lintab.htm>. (site consulted on April 28, 2008).
- Schroeder, J., 1977. Les formes de glace des grottes de la Nahanni, T.N.O., Canada. *Canadian Journal of Earth Sciences* 14, 1179–1185.
- Schweingruber, F.H., 1983. *Der Jahring. Standort, Methodik, Zeit und Klima in der Dendrochronologie*. Paul Haupt, Bern.
- Schwikowski, M., Barbante, C., Döring, T., Gäggeler, H.W., Boutron, C., Schotterer, U., Tobler, L., Van de Velde, K., Ferrari, C., Cozzi, G., Rosman, K., Cescon, P., 2004. Post-17th-century changes of European lead emissions recorded in high-altitude Alpine snow and ice. *Environmental Science and Technology* 38, 957–964.
- Sjögren, P., 2006. The development of pasture woodland in the southwest Swiss Jura Mountains over 2000 years, based on three adjacent peat profiles. *The Holocene* 16 (2), 210–223.
- Söderström, L., 1988. Sequence of bryophytes and lichens in relation to substrate variables of decaying coniferous wood in Northern Sweden. *Nordic Journal of Botany* 8, 89–97.
- Stoffel, M., Bollschweiler, M., 2008. Tree-ring analysis in natural hazards research – an overview. *Natural Hazards and Earth System Sciences* 8, 187–202.
- Stoffel, M., Conus, D., Grichting, M.A., Lièvre, I., Maître, G., 2008. Unraveling the patterns of late Holocene debris-flow activity on a cone in the central Swiss Alps: chronology, environment and implications for the future. *Global and Planetary Change* 60, 222–234.
- Stokes, M.A., Smiley, T.L., 1968. *An Introduction to Tree-ring Dating*. University of Chicago Press, Chicago.
- Storaunet, K.O., Rolstad, J., 2004. How long do Norway spruce snags stand? Evaluating four estimation methods. *Canadian Journal of Forest Research* 34, 376–383.
- Storaunet, K.O., Rolstad, J., 2002. Time since death and fall of Norway spruce logs in old-growth and selectively cut boreal forest. *Canadian Journal of Forest Research* 32, 1801–1812.
- Vaganov, E.A., Hughes, M.K., Shashkin, A.V., 2006. *Growth Dynamics of Conifer Tree Rings. Images of Past and Future Environments*. Springer, Berlin.
- van der Knaap, W.O., Leeuwen, J.F.N., Finsinger, W., Gobet, E., Pini, R., Schweizer, A., Valsecchi, V., Wick, L., Ammann, B., 2005. Migration and population expansion of *Abies*, *Fagus*, *Picea* and *Quercus* since 15'000 years in and across the Alps, based on

- pollen-percentage threshold values. *Quaternary Science Reviews* 24 (5–6), 645–680.
- Vogel, J.S., Southon, J.R., Nelson, D.E., Brown, T.A., 1984. Performance of catalytically condensed carbon for use in accelerator mass spectrometry. *Nuclear Instruments and Methods in Physics Research B* 5 (2), 289–293.
- Wigley, T.M.L., Briffa, K.R., Jones, P.D., 1984. On the average value of correlated time series, with applications in dendroclimatology and hydrometeorology. *Journal of Climate and Applied Meteorology* 23, 201–203.
- Yonge, C.J., MacDonald, W.D., 1999. The potential of perennial cave ice in isotope palaeoclimatology. *Boreas* 28, 357–362.